IMEKO International Conference on
Metrology for Archaeology and Cultural Heritage
Torino, Italy, October 19-21, 2016

Performance evaluation and experimental characterization of a new automatic method for measuring vertebrae

L. Di Angelo, P. Di Stefano

Department of Industrial and Information Engineering, and of Economics – University of L'Aquila, via G. Gronchi 18 L'Aquila, Italy, {luca.diangelo,paolo.distefano}@univaq.it

***Abstract* – In this paper performance evaluation and experimental characterization of a new automatic method for measuring vertebrae are analysed. Starting to a discrete valid geometric model of the vertebra, obtained from CT-scans or 3D scanning, the method measures algorithmically vertebrae. The proposed study is performed by analysing the most used dimensional features of lumbar and thoracic real vertebrae in anthropological investigations. The results are compared with the state-of-the-art methods for vertebra measurement.**

I. INTRODUCTION AND RELATED WORKS

Some geometric and dimensional parameters of the human vertebrae are usually analysed to gather some evidences useful in different fields. These dimensional features are used in related literature in the anthropological and forensic investigations for body mass estimation [1], identification of the height, posture and locomotion mode of a subject [1], gender, age and ethnicity of the subject ([2] and [3]). In every previously described applications, measures are required to be accurate enough to discriminate the factor being investigated.

The measurements on real vertebrae are commonly performed with a sliding caliper and a goniometer. However, in the last few years, the Coordinate Measure Machines (CMM) are being widely used too. When the vertebra is available in the form of a 3D geometric model (as it is the case of CT-scans) its measurement is performed as point-to-point distance between points manually selected by the operator in a specific software. All these approaches to vertebra measurement are affected by wide uncertainties. At the purpose to reduce the measurement uncertainties, recently, the authors presented a new automatic approach to measure vertebra starting from a 3D model of the vertebra obtained from CT-scans or 3D scanning [4]. A similar approach has been proposed to measure automatically the most important dimensional features detectable in teeth [].

In this paper, the *intra-tester repeatability* and *inter-tester reproducibility* of the contact methods are compared with those of a new method [4]. The performance evaluation and experimental characterization of methods are performed by analysing the most significant measuring features of real vertebrae.

II. MATERIALS AND METHODS

The human vertebrae can be classified into three main categories: lumbar, dorsal and cervical. In this paper, the lumbar and thoracic vertebrae are considered, since they have a similar morphology and the same dimensional features. The most used dimensional features of the lumbar and thoracic vertebrae in anthropological investigations are:

- *Spinous process length* (*spl*) ([6]);
- *Spinous process angle* (*spa*) ([7]);
- *Superior and inferior vertebral body length (svbl and ivbl) ([3]);*
- *Superior and inferior vertebral body width (svbw and ivbw) ([3]);*
- *Anterior and posterior lateral vertebral body height (avbh and pvbh) ([3]);*
- *Vertebral canal length (vcl) ([8]);*
- *Vertebral canal breadth (vcb) ([8]).*

A. Traditional contact methods

The traditional methods used to measure the dimensional features, here analysed, are those with sliding caliber and CMM machine. In this paper, the measurements with CMM are carried out by the 7-axis Faro Edge contact measurement system with 3-mm zirconia ball i-probe (Faro Company, USA, accuracy of 0.029 mm). Fig. 1 reports the definitions of measurement by using these methods.

B. The new automatic method

The new automatic method proposed in [4] requires a 3D discrete model of the vertebra obtained from CT-scans or 3D scanning. In this paper, the 3D point acquisition of the data is carried out by a calibrated FARO® Edge, 9 ft (2.7m) laser scanner (where the single point repeatability

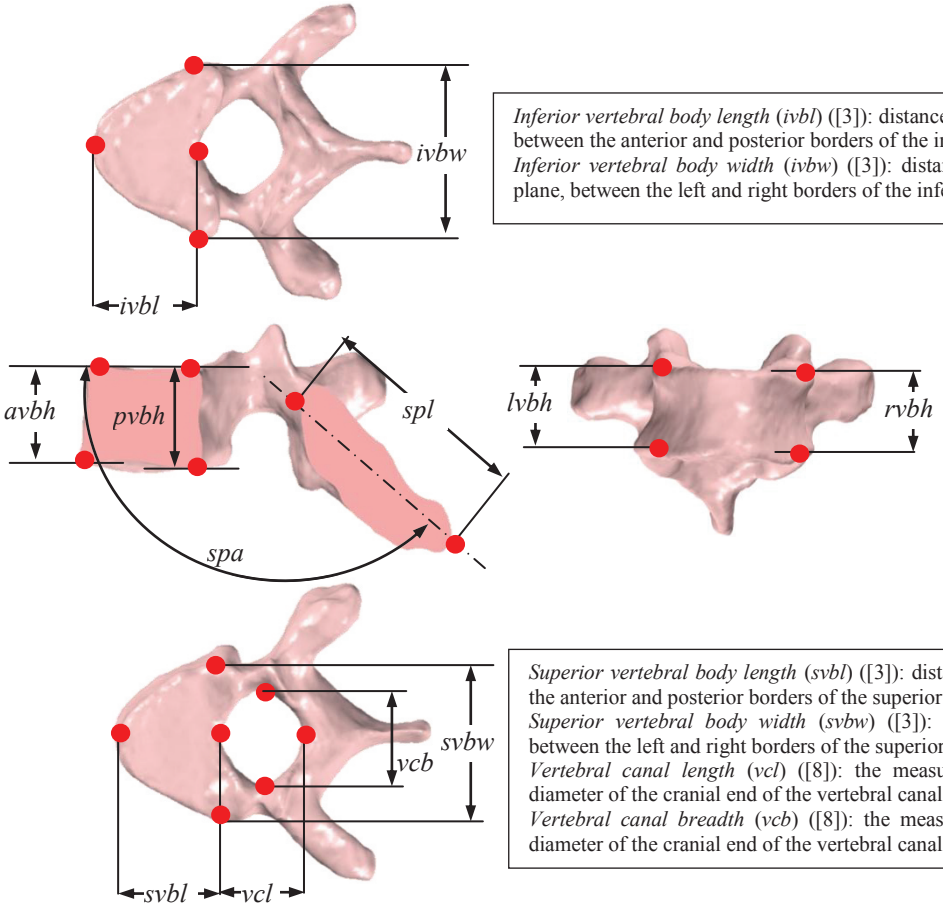

Inferior vertebral body length (*ivbl*) ([3]): distance, in the sagittal plane, between the anterior and posterior borders of the inferior vertebral body.
Inferior vertebral body width (*ivbw*) ([3]): distance, in the transverse plane, between the left and right borders of the inferior vertebral body.

Spinous process length (*spl*) ([6]): Distance, along the axis of the spinous process, between the posterior-most point of the superior border of the vertebral canal at the midline and the distal-most tip of the spinous process.
Spinous process angle (*spa*) ([7]): Angle between the midline of the cranial end of the body and the cranial edge of the spinous process.
Anterior and posterior lateral vertebral body height (*avbh* and *pvbh*) ([3]): distance, in the sagittal plane, between the central borders of the superior and inferior vertebral body, anteriorly and posteriorly, respectively.
Left and right lateral vertebral body height (*lvbh* and *rvbh*) ([3]): distance, in the frontal plane, between the superior and inferior lateral vertebral body borders.

Superior vertebral body length (*svbl*) ([3]): distance, in the sagittal plane, between the anterior and posterior borders of the superior vertebral body.
Superior vertebral body width (*svbw*) ([3]): distance, in the transverse plane, between the left and right borders of the superior vertebral body.
Vertebral canal length (*vcl*) ([8]): the measure of the maximum dorsoventral diameter of the cranial end of the vertebral canal.
Vertebral canal breadth (*vcb*) ([8]): the measure of the maximum mediolateral diameter of the cranial end of the vertebral canal.

Figure 1. The measuring features of the vertebra

is certified by the manufacturer from 0.024mm to 0.064mm and the average point spacing of the point cloud has been set to 0.1 mm). The processing of point cloud for the generation of the geometric model needs some interaction with the operator (figure 2):

- points clouds filtering;
- points clouds registration;
- points cloud tessellation and error rectification.

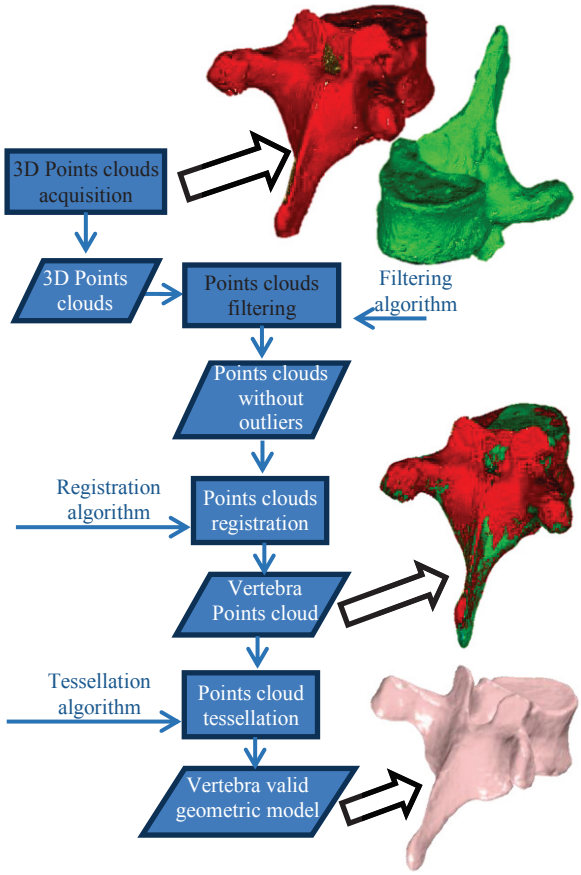

Fig. 2. Flow chart of point cloud processing for the generation of a 3D discrete valid geometric model

These procedures, with the exception of point cloud registration processes are, however, codified and, consequently, easily reproducible and repeatable. This phase is mandatory since the whole vertebra cannot be scanned in only process, but require that two or more point cloud are registered each other. In this paper, the registration is performed by the classical *ICP* method.

Once a valid geometric model is available, the method analyses a vertebra in algorithmically, without any interaction with the operator. Firstly, the method performs a preliminary identification of six derived geometric features of the vertebra (figure 3):

- The *symmetry plane* Π_S of the vertebra detected in according to the method proposed in [9]];
- The *vertebral cylinder* Ω (radius r_c and axis $\mathbf{a}_c$), approximating the vertebral foramen *VF*:
- The *coronal plane* Π_C, which divides the vertebra into the *body* and the *posterior element*;
- The *middle plane* Π_M of the body;
- The *second coronal plane* Π_B, which is assumed to be the plane which is perpendicular to the *symmetry plane* and partitions the *body* of the vertebra;
- The *axis of the posterior spinous process* $\mathbf{a}_s$.

These geometric entities are constrained by one another as follows:

$$\Pi_C, \Pi_B, \Pi_M \perp \Pi_S \; ; \; \Pi_M \perp \Pi_B$$
$$\mathbf{a}_C \equiv \Pi_S \cap \Pi_C \; ; \; \mathbf{a}_S \in \Pi_S \qquad (1)$$

The rules to detect each of above-mentioned derived geometric features are reported in [4].

Once the characteristic planes are detected, the dimensional features of the vertebra can be evaluated. The Figure 4 reports the rules for the identification of the dimensional features here considered. The dimensional features are grouped together according to the characteristic plane on which they are identified.

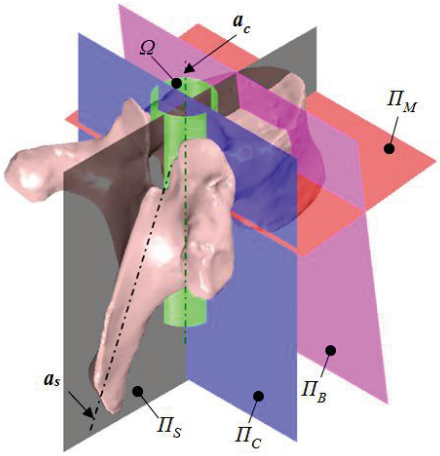

Fig. 3. The main geometric features of a vertebra.

C. The sample of vertebrae

In order to characterize the methods, a set of eight vertebrae (five thoracic, labelled from *T1* to *T5* and three lumbar labelled from *L1* to *L3*) have been used. These vertebrae are randomly selected from three non-pathological complete adult skeletons. An experienced spinal researcher has visually inspected each vertebra in order to exclude pathological diseases.

III. RESULTS AND CONCLUSION

Since any measurement uncertainties in the dimensional features result from the contribution of both *intra-tester repeatability* and *inter-tester reproducibility*, in this paper a specific experimentation is carried out to analyse these two components of measurement error.

The testers are 12 medical students, in the fifth year of their medical course and onwards, trained appropriately.

Let us consider, then, that the *intra-tester repeatability* and the *inter-tester reproducibility* of the measurements have been made according to the corresponding previously reported protocols. Nonetheless, all the testers have been blinded to the results of the measurements. Each set of measures has been subjected to the Kolmogorov-Smirnov test to check whether the data is normally distributed. In this case, the P values recorded are, in all cases, higher than 0.05, which indicates a normal distribution of all variables.

In order to evaluate the *Intra-tester repeatability* (*TRA*) of the traditional methods (*C&G* and *CMM*), each of the 12 testers have performed 20 measures for each dimensional feature of eight vertebrae, under repeatability experimental conditions. Regarding to the new automatic method (*AQ*), each vertebra has been scanned 20 times, under the same operative conditions by same operators and each 3D geometric model has been processed by the software implementation of the proposed method. In any cases, the *Intra-tester repeatability* (*TRA*) is evaluated as the standard deviation of the 20 performed measures for each vertebra and geometrical feature. In the table 1, by way of example, the mean values of *TRA* for the vertebrae labelled *T1* and *L1* are reported. However, similar values have been found for the other vertebrae. The repeatability of traditional methods in the dimensional features, in many cases does not permit to discriminate the factor being investigated. Regarding the *AQ* method, since the parameters are calculated algorithmically, the *Intra-tester repeatability* is affected mainly by the point cloud registration process, rate sample of the model and the measuring noise. The repeatability of the *AQ* method is, in any of the tested cases, greater than that observed in the traditional methods (C&G and CMM). The repeatability of the geometrical features, intrinsically more complicated to measure with traditional methods (such as *spl* and *spa*), is of the same order of magnitude of the other ones.

In order to evaluate the *inter-tester reproducibility* of the traditional methods, each of the 12 testers evaluates the dimension of the feature as the mean value of three measurements. Concerning the *AQ* method, each vertebra has been acquired three times and each geometric model processed. In any cases, the *inter-tester reproducibility* (*TER*) is evaluated as the standard deviation of the 12 measures performed for each dimensional feature by the different testers. The degree of reproducibility reached through the proposed method is higher than that shown through the other methods for all the dimensional features: it is on average 6 times lower than with the C&G (table 2). Table 3 reports the mean values of the measures for *T1* and *L1* taken with the three methods. Wide differences can be observed which are mainly due to the different measuring protocols used for each method that follows a different criterion for identifying the measuring references. Therefore, there is no identifiable reference value of the measure for an accurate evaluation.

Since any measurement uncertainties in the dimensional features result from the contribution of both *intra-tester repeatability* and *inter-tester reproducibility*, the carried out experimentation shows, as the proposed method is more accurate than the state-of-the-art. The high accuracy of the method and the objective measures, which it provides, may open up the road to new investigations in anthropology. Furthermore, due to the comparatively shorter time required for the scanning process and for the next data processing, the proposed method makes it possible to process a relatively large number of vertebrae quickly and easily, without an operator with special skills, such as an anthropologist or an anatomist.

REFERENCES

[1] E. White T.D., M. Black, T., Folkens, P.A., 2000. Human Osteology, second ed., Academic Press, San Diego.

[2] Masharawi, Y., Salame, K., 2011. Shape variation of the neural arch in the thoracic and lumbar spine: characterization and relationship with the vertebral body shape. Clin Anat 24, 858–867.

[3] Zheng, W.X., Cheng, F.B., Cheng, K.L., Tian, Y., Lai, Y., Zhang, W.S., Zheng, Y.J., Li Y.Q., 2012. Sex assessment using measurements of the first lumbar vertebra. Foren. Science Intern. 219, 285.e1–285.e5.

[4] Di Angelo, L., Di Stefano P., 2015. A new method for the automatic identification of the dimensional features of vertebrae. Computer Methods and Programs in Biomedicine 121, 36-48.

[5] Di Angelo, L., Di Stefano, P., Bernardi, S., Continenza, M.A., 2016. A new computational method for automatic dental measurement: The case of maxillary central incisor. Computers in Biology and Medicine 70, 202-206.

[6] O'Higgins, P., Milne, N., Johnson, D.R., Runnion, C.K., Oxnard, C.E., 1997. Adaptation in the vertebral column: A comparative study of patterns of metameric variation in mice and men. Journal of Anatomy 190, 105–113.

[7] Latimer, B., Ward, C. V., 1993. The thoracic and lumbar vertebrae. In: A. Walker and R. Leakey (Eds.) The Nariokotome Homo erectus skeleton. Cambridge, MA: Harvard Univ. Press, pp. 266–293.

[8] Martin, R., 1928. Lehrbuch der Anthropologie in Systematischer Darstellung mit Besonderer Berücksichtigung der anthropologischen Methoden für Studierende, Ärtze und Forschungsreisende, vol. 2: Kraniologie, Osteologie. Jena, Germany: Gustav Fischer. pp 345-355.

[9] Di Angelo, L., Di Stefano P., 2014. A computational Method for Bilateral Symmetry Recognition in Asymmetrically Scanned Human Faces. Computer-Aided Design and Applications,. 11 (3), 275-283.

Measurements on sagittal plane

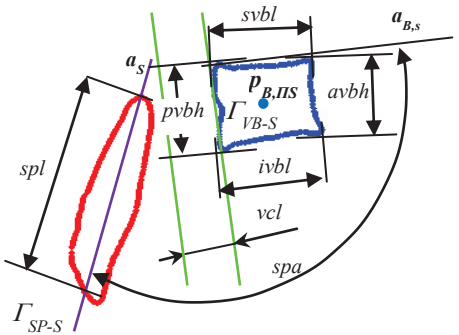

vcl is assumed to be the minimum distance between the points pertaining to $\Gamma_{VB\text{-}S}$ and $\Gamma_{SP\text{-}S}$
spl is conventionally evaluated along the $\mathbf{a_S}$ direction
spa is calculated as the angle between $\mathbf{a_s}$ and $\mathbf{a_{B,s}}$
svbl (*ivbl*) is the largest distance between the upper (lower) portion of the anterior and posterior part of $\Gamma_{VB\text{-}S}$, whose dimension line is parallel to $\mathbf{a_{B,s}}$.
pvbh (*avbh*) is the largest distance between the posterior (anterior) portion of $\mathbf{a_{B,s}}$ and $\mathbf{a_{B,i}}$, whose dimension line is perpendicular to $\mathbf{a_{B,m}}$.

Measurements on coronal planes

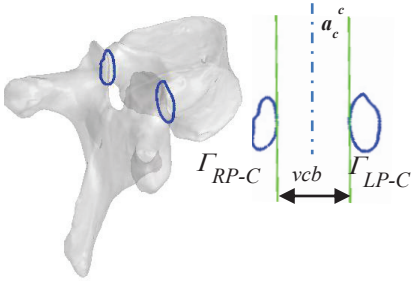

vcb is assumed to be the minimum distance between the points pertaining to $\Gamma_{LP\text{-}C}$ and $\Gamma_{RP\text{-}C}$, whose dimension line is perpendicular to the projection of $\mathbf{a_c}$ onto Π_C ($\mathbf{a_c^c}$)

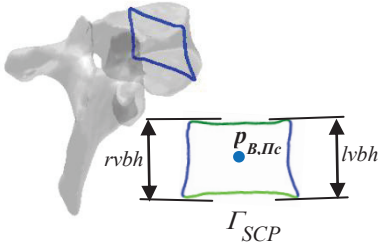

lvbh (*rvbh*) is the maximum height of the left (right) portion of Γ_{SCP} (intersection between the vertebra and Π_B), whose dimension line is perpendicular to Π_M.

Measurements by middle plane

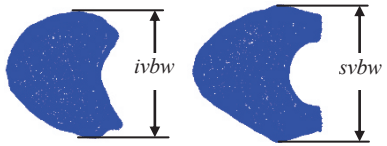

svbw (*ivbw*) is the largest distance, measured parallel to the *coronal plane*, between all the body points which are over (under) the *middle plane* and projected onto Π_M.

Figure 4. Rules for the determination of the parameters with the proposed method.

Table 1. Comparison of intra-tester repeatability

		Spinous Process		Body								Vertebral canal	
vertebra	**Method**	TRA_{spl}	TRA_{spa}	TRA_{svbl}	TRA_{svbw}	TRA_{ivbl}	TRA_{ivbw}	TRA_{lvbh}	TRA_{rvbh}	TRA_{avbh}	TRA_{pvbh}	TRA_{vcb}	TRA_{vcl}
T1	*AQ*	0.11	0.17	0.05	0.10	0.20	0.08	0.18	0.16	0.12	0.12	0.05	0.14
	C&G	0.41	7.63	0.24	0.38	0.23	0.38	0.19	0.54	0.09	0.25	0.26	0.26
	CMM	1.58	5.37	0.58	0.96	0.88	0.74	0.56	0.66	0.44	0.66	0.88	0.91
L1	*AQ*	0.07	0.15	0.08	0.05	0.21	0.15	0.16	0.15	0.10	0.09	0.15	0.09
	C&G	0.59	7.10	0.36	0.31	0.22	0.25	0.38	0.38	0.28	0.43	0.15	0.28
	CMM	1.31	6.69	0.36	0.55	0.27	0.52	0.30	0.67	0.17	0.60	0.16	0.77

Table 2. Comparison of inter-tester reproducibility

		Spinous Process		Body								Vertebral canal	
vertebra	**Method**	TER_{spl}	TER_{spa}	TER_{svbl}	TER_{svbw}	TER_{ivbl}	TER_{ivbw}	TER_{lvbh}	TER_{rvbh}	TER_{avbh}	TER_{pvbh}	TER_{vcb}	TER_{vcl}
T1	*AQ*	0.20	0.18	0.14	0.10	0.07	0.08	0.19	0.18	0.12	0.14	0.08	0.16
	C&G	0,46	8,30	0,21	1,35	0,13	0,47	0,25	0,61	0,13	0,16	0,31	0,33
	CMM	1.90	3.95	0.70	1.32	0.59	0.66	0.44	0.47	0.47	0.58	1.32	1.62
L1	*AQ*	0.24	0.32	0.18	0.20	0.11	0.19	0.10	0.12	0.16	0.11	0.16	0.18
	C&G	2,02	13,71	0,41	0,35	0,10	0,27	0,39	0,39	0,20	0,43	0,17	0,67
	CMM	0.52	6.80	0.45	0.45	0.16	0.50	1.09	0.85	0.11	0.76	0.18	0.70

Table 3. Comparison of the mean value of the obtained measures

		Spinous Process		Body								Vertebral canal	
vertebra	**Method**	μ_{spl}	μ_{spa}	μ_{svbl}	μ_{svbw}	μ_{ivbl}	μ_{ivbw}	μ_{lvbh}	μ_{rvbh}	μ_{avbh}	μ_{pvbh}	μ_{vcb}	μ_{vcl}
T1	*AQ*	44.44	108.29	20.56	29.11	20.61	28.11	16.64	17.21	15.67	17.81	14.08	13.16
	C&G	44.44	121.14	20.28	28.24	20.95	27.74	17.90	17.61	15.87	18.56	14.11	13.23
	CMM	44.51	115.73	22.48	30.62	22.77	30.28	21.25	20.45	18.41	21.09	12.35	12.92
L1	*AQ*	27.94	139.21	28.59	42.68	28.66	46.13	23.18	22.91	22.64	24.05	18.70	12.73
	C&G	27.19	145.05	29.09	43.09	28.95	46.15	23.07	23.37	22.78	25.07	18.54	12.85
	CMM	28.20	152.88	31.69	45.54	31.93	48.57	25.59	26.05	25.55	27.18	15.47	11.16